Available online at www.sciencedirect.com
ScienceDirect
Atmospheric Environment 41 (2007) 1251–1266
ATMOSPHERIC ENVIRONMENT
www.elsevier.com/locate/atmosenv

The impact of transpacific transport of mineral dust in the United States

T. Duncan Fairlie[a,b,*], Daniel J. Jacob[b], Rokjin J. Park[b]

[a]*NASA Langley Research Center, Hampton, VA 23681, USA*
[b]*Department of Earth and Planetary Sciences and Division of Engineering, Harvard University, Cambridge, MA 02138, USA*

Received 1 May 2006; received in revised form 20 September 2006; accepted 22 September 2006

Abstract

We use a global chemical transport model (GEOS-Chem) to estimate the impact of transpacific transport of mineral dust on aerosol concentrations in North America during 2001. We have implemented two dust mobilization schemes in the model (GOCART and DEAD) and find that the best simulation of North American surface observations with GEOS-Chem is achieved by combining the topographic source used in GOCART with the entrainment scheme used in DEAD. This combination restricts dust emissions to year-round arid areas but includes a significant wind threshold for dust mobilization. The model captures the magnitude and seasonal cycle of observed surface dust concentrations over the northern Pacific. It simulates the free tropospheric outflow of dust from Asia observed in the TRACE-P and ACE-Asia aircraft campaigns of spring 2001. It reproduces the timing and distribution of Asian dust outbreaks in North America during April–May. Beyond these outbreaks we find persistent Asian fine dust (averaging $1.2\,\mu g\,m^{-3}$) in surface air over the western United States in spring, with much weaker influence ($0.25\,\mu g\,m^{-3}$) in summer and fall. Asian influence over the eastern United States is 30–50% lower. We find that transpacific sources accounted for 41% of the worst dust days in the western United States in 2001.

Keywords: Transpacific; Transport; Mineral; Dust

1. Introduction

Mineral dust is a large contributor to aerosol loading in the Earth's atmosphere (Penner et al., 2001) with important implications for air quality, climate, atmospheric chemistry, and the biosphere. Airborne fine dust ($<2.5\,\mu m$ diameter) has a particularly harmful effect on the human respiratory system (Dockery et al., 1993), and adversely impacts visibility (Malm et al., 2000). Scattering and absorption by dust impact the Earth's radiation budget (Sokolik et al., 2001), the thermal structure of the troposphere, and actinic fluxes (Liao et al., 1999), altering dynamical, and photochemical processes. Coating of dust particles under polluted conditions (Clarke et al., 2004) can change microphysical properties and promote surface chemical processes (Dentener et al., 1996; Jacob, 2000). Dust deposits minerals to the oceans and to the terrestrial

*Corresponding author. NASA Langley Research Center, Hampton, VA 23681, USA. Tel.: +1 757 864 5818; fax: +1 757 864 6326.
E-mail address: t.d.fairlie@larc.nasa.gov (T. Duncan Fairlie).

1352-2310/$ - see front matter © 2006 Elsevier Ltd. All rights reserved.
doi:10.1016/j.atmosenv.2006.09.048

biosphere (Fung et al., 2000; Meskhidze et al., 2005) while fungal spores are transported on dust particles across oceans (Shinn et al., 2000).

Mineral dust is mobilized by strong winds over arid terrains. Principal source regions are deserts or dry lakes and streambeds where alluvial deposits have accumulated (Ginoux et al., 2001; Prospero et al., 2002). Natural sources are thought to be dominant, but human activity can also contribute (Tegen et al., 2004; Mahowald et al., 2004). Most airborne dust falls out close to the source but fine dust can be transported over long distances: from North Africa to the Caribbean and Florida (Perry et al., 1997; Prospero, 1999) and from Asia to North America (Husar et al., 2001; Jaffe et al., 1999).

Mineral dust is usually a small component of aerosol loading in the United States (EPA, 2003), but occasionally it can raise aerosol concentrations above EPA air quality standards during domestic and overseas events (Husar et al., 2001; Jaffe et al., 2003; Szykman et al., 2003; Prospero, 1999). It also impacts the Regional Haze Rule (RHR) of the US Environmental Protection Agency (EPA, 2003), which requires states to develop implementation plans for achieving "natural visibility conditions" at class 1 sites (national parks, monuments, and wilderness areas) by 2064. Defining natural visibility objectives requires improved understanding of natural aerosol sources, and the impact of transboundary contributions. Park et al. (2004) found that trans-Pacific transport of Asian sulfate pollution will prevent natural visibility goals from being attained. Here, we examine the effect of overseas dust. The occurrence of springtime Asian dust events at US sites is well known (Jaffe et al., 1999). More recently, cluster analysis of surface elemental data taken at Interagency Monitoring for Protected Visual Environments (IMPROVE) sites in the United States has suggested that Asian dust is pervasive over North America, extending beyond sporadic springtime episodes (Van Curen & Cahill, 2002). This study is designed to assess the contribution of Asian dust over the United States and its impact on RHR goals.

2. Methodology

We have conducted global annual dust simulations for 2001 using the GEOS-Chem chemical transport model (CTM) (Bey et al., 2001; Park et al., 2004) to describe the mobilization, transport and deposition of mineral dust in the atmosphere. Separate simulations were conducted to distinguish contributions from overseas and domestic dust sources to North America.

2.1. Model description

GEOS-Chem is a global CTM driven by GEOS assimilated meteorological fields from the NASA Goddard Modeling and Assimilation Office (GMAO). The GEOS-3 fields for 2001 have $1^\circ \times 1^\circ$ horizontal resolution, and 48 vertical *sigma* levels extending from the surface to approximately 0.01 hPa. We degrade them to $2^\circ \times 2.5^\circ$ for input to GEOS-Chem.

The mineral dust module in GEOS-Chem describes the mobilization of dust from the Earth's surface, gravitational settling, and wet and dry deposition. For the simulations presented here, the dust is distributed in four-size bins (radii 0.1–1.0, 1.0–1.8, 1.8–3.0, and 3.0–6.0 μm), following Ginoux et al. (2004). Dry deposition is represented with a deposition velocity that accounts for gravitational settling (Seinfeld and Pandis, 1998) and turbulent dry transfer of particles to the surface (Zhang et al., 2001). Wet deposition uses the scheme of Liu et al. (2001), which includes scavenging in convective updrafts, rainout and washout from large-scale precipitation and convective anvils.

2.2. Dust mobilization

Mobilization of soil particles from the Earth's surface takes place when the turbulent drag of the atmosphere overcomes gravitational inertia and inter-particle cohesion. Only clay and silt particles (diameters: $<2.5\,\mu m$, and $2.5<D<60\,\mu m$, respectively) remain airborne for more than a few minutes (Marticorena and Bergametti, 1995, hereafter MB95). These particles are difficult to mobilize directly, because of cohesive forces (Iversen et al., 1976), but are liberated by bombardment by larger (saltating) sand particles ($D>60\,\mu m$).

We implemented two dust mobilization schemes in GEOS-Chem: (1) the scheme of Ginoux et al. (2004, hereafter G04), developed for the GOCART CTM and (2) the dust entrainment and deposition (DEAD) scheme of Zender et al. (2003a, b hereafter Z03a,b). Both schemes treat the vertical dust flux as proportional to the horizontal saltation flux. The DEAD scheme (Z03) follows MB95 in computing a total horizontal saltation flux, Q_s, based on the

theory of White (1979):

$$Q_s = C_z \frac{\rho_{air}}{g} U^{*3} \left(1 - \frac{U_t^*}{U^*}\right)\left(1 + \frac{U_t^*}{U^*}\right)^2, \quad (1)$$

where U^* is the friction velocity, $U_t^*(D)$ is the threshold friction velocity, ρ_{air} is the air density, g is the acceleration of gravity, and C_Z is a global tuning factor. Q_s is computed at $D = 75\,\mu m$, where U_t^* is a minimum, and the total vertical dust flux is given by

$$F = A_m S_z \alpha Q_s, \quad (2)$$

where the sandblasting mass efficiency, α, depends on the fraction M_{clay} of clay in the soil, A_m is the fractional area of land suitable for mobilization, and S_z is the "erodibility," an efficiency factor that favors emissions from specified geographic features. We followed Z03b in using "geomorphic erodibility," which depends on upstream runoff area, and set $M_{clay} = 0.2$ globally. We computed U^* from the 10-m wind speed assuming neutral stability below and used a roughness length $Z_0 = 100\,\mu m$, recommended by Z03a for dust mobilization candidate cells. F is distributed by particle size as a globally uniform tri-modal lognormal probability density function, which we project on to the selected size bins specified above.

The GOCART scheme (G04) follows Gillette and Passi (1988) in computing a size segregated vertical dust flux, F_p, for each size class, p:

$$F_p = C_G S s_p U_{10}^2 (U_{10} - U_t^*), \quad (3)$$

where the "source function," S, serves the same role as the product $A_m S_z$ in DEAD (Eq. (2)), s_p is the mass fraction applied to each size class, U_{10} is the 10-m wind speed, and C_G is a global constant. S confines dust emissions to topographic depressions in desert and semi-desert areas of the world (Ginoux et al., 2001, hereafter G01) and is time invariant.

Soil moisture, vegetation, rocks and stones, and snow cover inhibit dust mobilization by contributing to cohesion, by shielding the surface and acting as a momentum sink on the flow. Both schemes represent the impact of soil moisture by increasing U_t^*. In GOCART emissions are completely shut off when the surface volumetric water content θ exceeds $0.2\,m^3\,m^{-3}$. In DEAD, moisture inhibition becomes important when θ exceeds $0.3\,m^3\,m^{-3}$. Because U_t^* is of similar magnitude to U^* but an order of magnitude smaller than U_{10}, the wind threshold under dry conditions, for a given meteorological forcing, is significant in DEAD but is negligible in GOCART.

Although the DEAD and GOCART schemes differ in detail, they differ most fundamentally in representing the role of vegetation. GOCART restricts emissions to persistent arid regions, whereas DEAD permits regions that become seasonally devegetated to mobilize. The mobilization land fraction for DEAD

$$A_m = (1 - A_s)(1 - A_l - A_w)(1 - A_v) \quad (4)$$

(refer Eq. (2)) comprises factors that suppress dust emission from snow-covered ground, wetlands and bodies of water, and vegetated areas, respectively. The vegetation term $(1-A_v)$ uses monthly mean leaf plus stem area index (LAI) diagnosed from AVHRR data, and decreases linearly from 1 to 0 as LAI increases from 0 to 0.3 (Z03a).

2.3. A combined mobilization scheme for GEOS-Chem

The performance of a mobilization scheme in a CTM depends on the model is sensitive to the meteorological fields used, and the data set used for evaluation (Cakmur et al., 2006). Modelers typically use global factors (e.g., C_G and C_Z above) to tune dust emissions to optimize comparisons to a particular set of measurements (e.g., Mahowald et al., 2002). Here, we are particularly concerned with the performance of the model with respect to North American surface observations, and to transpacific transport. Full-year mineral dust simulations were conducted for 2001 using both the GOCART and DEAD mobilization schemes, with total annual emissions for each simulation scaled to 1453 T_g, well within the range of estimated global dust emissions from models (Textor et al., 2006; Cakmur et al., 2006). The different approaches to the role of vegetation between the two schemes produced very different spatial and temporal distributions of emissions over North America. While GOCART emissions were restricted to desert regions in the southwest, DEAD emissions were more prominent in the central and northern prairies, where LAI falls below the threshold for mobilization in fall and early spring.

Fig. 1 shows a comparison between simulated and annual mean fine dust ($<2.5\,\mu m$) observations at IMPROVE sites in the continental United States for 2001. IMPROVE sites are located in class I areas throughout the United States (Malm et al., 1994; Sisler, 1996; Van Curen and Cahill, 2002; http://vista.cira.colostate.edu/improve). Elemental

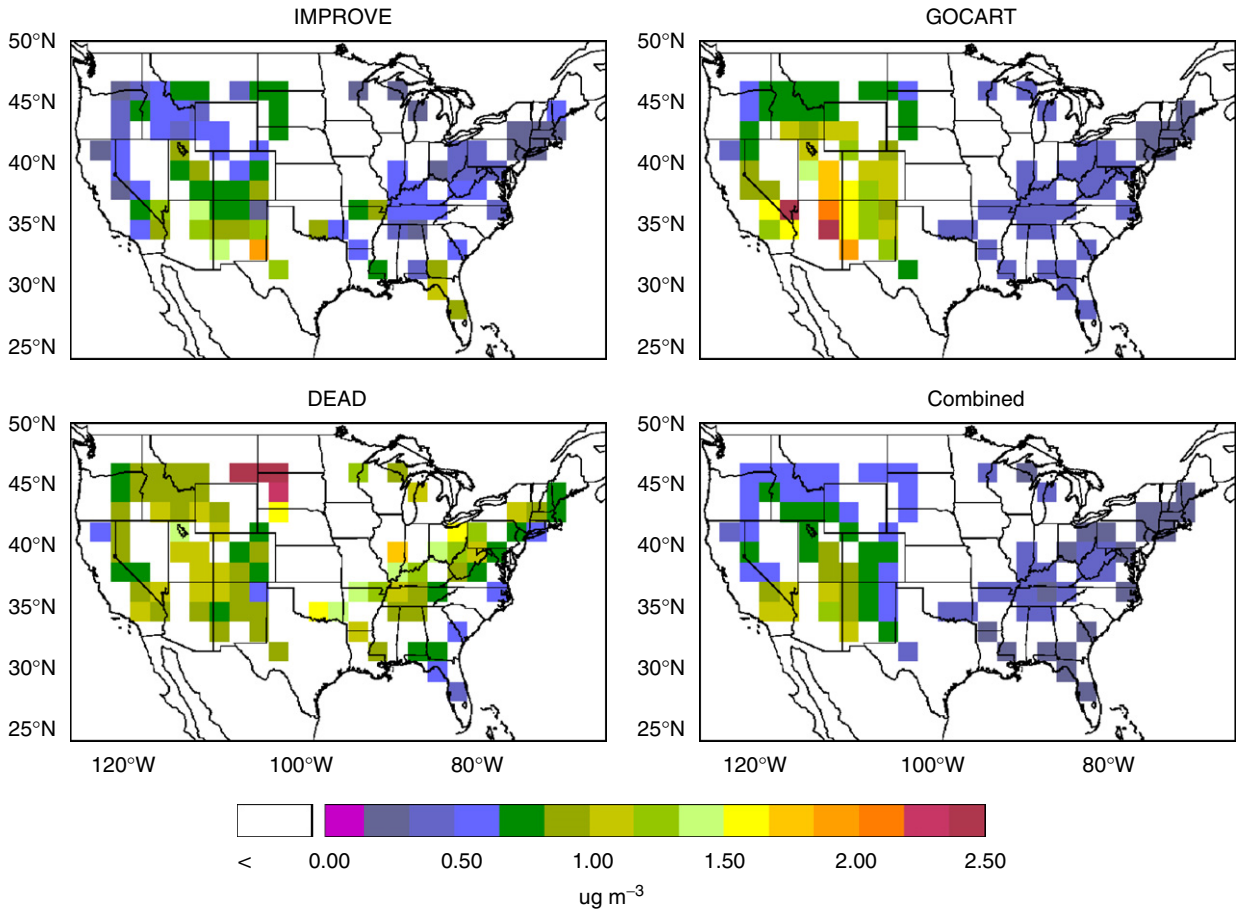

Fig. 1. Annual mean surface fine (<2.5 μm) dust concentrations (μg m^{-3}) in the United States for 2001. Model results using the GOCART, DEAD, and combined mobilization schemes are compared to observations from the IMPROVE network mapped over the model grid. Note: Color scale saturates at 2.5 μg m^{-3}; larger values appear red.

composition data are available every three days from 24-h samples; fine dust mass is estimated using the formula of Malm et al. (1994). The GOCART simulation shows good spatial representation of the observations ($r = 0.6$, mean bias = 0.17 μg m^{-3}, rms difference = 0.43 μg m^{-3}), but emissions in the west and southwest were found to be more prolonged than observations suggest, which we attribute to the low dry wind threshold in GOCART. Results with DEAD showed good spatial structure in the west, except that unrealistically large emissions were generated over the northern plains due to low LAI in fall and early spring, which propagated to eastern sites, resulting in a poorer overall comparison with IMPROVE ($r = 0.06$, mean bias = 0.41 μg m^{-3}, rms difference = 0.53). Although the plains can be a source of windblown dust, senescent and non-leafy vegetation, and soil conservation practices mitigate erosion (M. Black, Agriculture and Agri-Food, Canada, personal communication). LAI does not account for these factors.

These issues led us to combine the entrainment scheme used in DEAD with the source function, S, used in GOCART. The vertical dust flux is then given by

$$F = (1 - A_s) S \alpha Q_s \quad (5)$$

(cf. Eq. (2)). S restricts emissions to persistent desert and semi-desert regions, and $(1-A_s)$ retains suppression due to snow cover. Mahowald et al. (2002) and Luo et al. (2003) used similar approaches in their dust models. We find that this combination overcomes prolonged emissions in southwest (GOCART) and eliminates unrealistically strong emissions over the northern plains (DEAD), reducing regional mean biases and rms differences ($r = 0.55$,

mean bias = −0.09, rms difference = 0.26) (Fig. 1). The global annual emission remains at 1453 T_g. Hereafter, we use this combined scheme.

3. Global dust budget with combined scheme

Fig. 2 shows global maps of annual dust emission, dust loading, and dry and wet deposition from the 2001 simulation using the combined scheme. Table 1 shows the corresponding global, size-resolved dust budget. The maps of emission and loading clearly show the global "dust belt," which extends from North Africa, through the Middle East, into central Asia, China, and Mongolia (Prospero et al., 2002). Spring and early summer are the preferred times for emissions in both hemispheres. Easterly trade winds export North African dust to Central and South America in NH winter and spring, and the Caribbean in summer. Mid-latitude NH westerlies provide a pathway for Asian dust across the Pacific to North America. Except for NH winter, the model maintains an unbroken belt of dust loading exceeding 5 mg m^{-2} in northern mid-latitudes, and across the Pacific in particular.

Dry deposition is focused near the source regions, whereas wet deposition is more dispersed; high wet losses follow the ITCZ in the tropical Atlantic, and

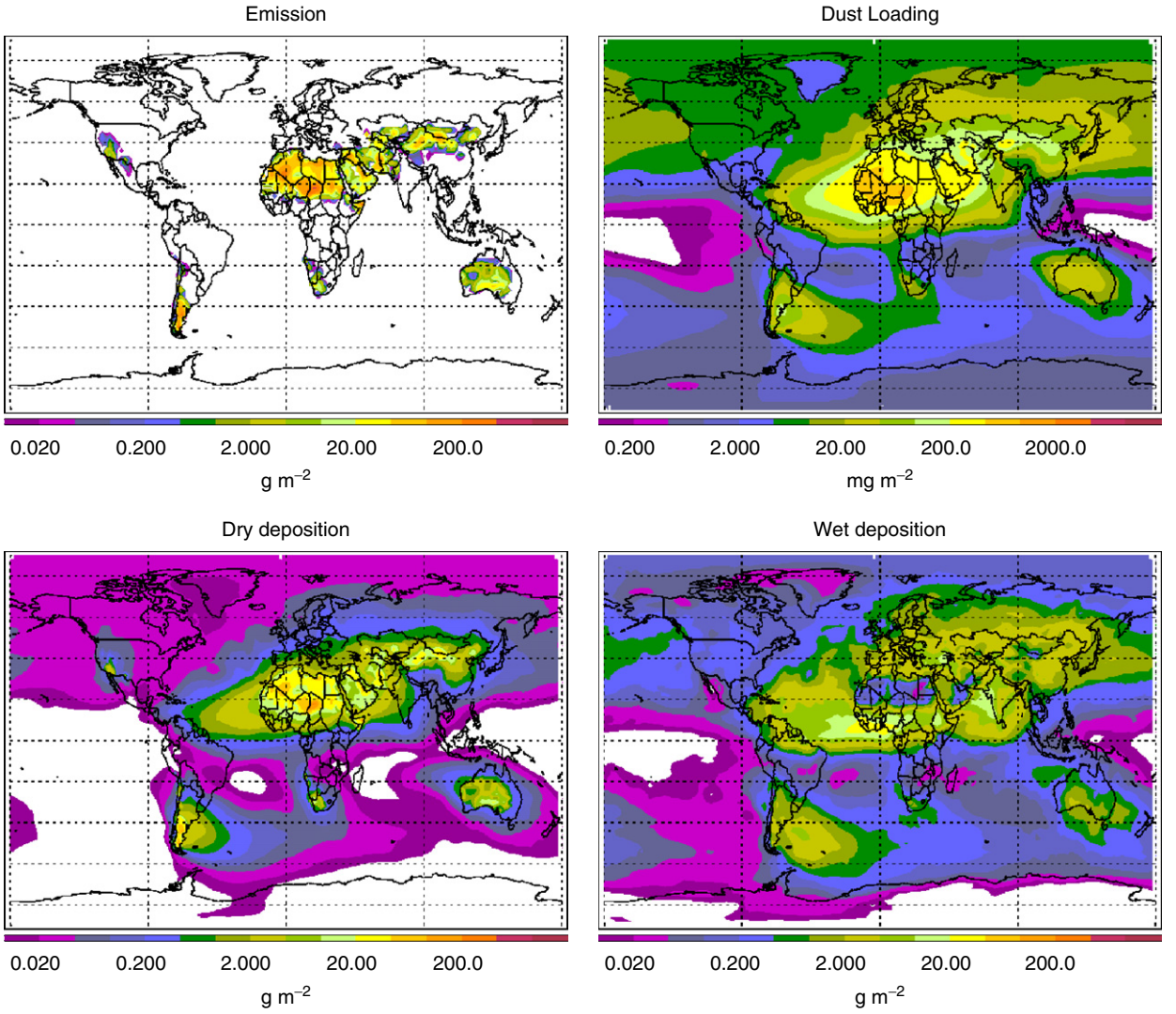

Fig. 2. Global maps of total annual dust emission (g m^{-2}), annual mean dust loading (mg m^{-2}), total dust mass dry deposited (g m^{-2}), and total dust mass wet deposited (g m^{-2}), for 2001 from the simulation.

Table 1
Global annual dust budget in the model

Radius range (μm)	Emission ($T_g\,yr^{-1}$)	Dry deposition ($T_g\,yr^{-1}$)	Wet deposition ($T_g\,yr^{-1}$)	Burden (T_g)	Lifetime (days)
0.1–1.0	178	44	134	3.9	8.3
1.0–1.8	368	126	241	6.9	6.9
1.8–3.0	469	278	188	5.4	4.3
3.0–6.0	439	393	43	1.4	1.2
Total	1453	841	604	17.6	5.1

mid-latitude storm tracks. Dry deposition accounts for 58% of dust mass loss. The 5.1-day overall lifetime and the relative wet and dry loss rates of dust in our model fall well within the extensive range of estimates from contemporary global models (Textor et al., 2006).

4. Evaluation of overseas dust sources

In this section we evaluate the ability of the model to reproduce dust observations relevant to assessing the overseas component of dust over North America. First, we use surface measurements at Northern Hemisphere sites for 2001 (when available) and other years. Then, since surface measurements may not be representative of Asian outflow and transpacific transport that occurs at higher altitudes, we focus on spring 2001 aircraft observations of Asian outflow over the western Pacific.

4.1. Northern hemisphere sites

We use a climatology of dust measurements from the worldwide network of ground stations managed by the University of Miami (Prospero, 1996). This data set has been used to evaluate previous global model simulations, e.g., G04, Z03, and Luo et al. (2003). Fig. 3 shows simulated and observed monthly mean dust concentrations at nine northern hemisphere sites. Data of 2001 for midway Island, Barbados, and Miami are included. Simulated values are selected at an altitude corresponding to the elevation of the surface observations. Observations at Cheju and Okinawa provide information on the seasonal cycle of dust generation and outflow from Asia. These stations show a springtime peak, and a secondary enhancement in the fall. Spring is the preferred season for dust mobilization and outflow in East Asia (Carmichael et al., 1996). April and May data show considerable interannual variability, attributed to variability of large-scale flow patterns by Zhang et al. (2003). A summertime lull at Cheju and Okinawa is associated with a more northeastward track for dust export from East Asia, with prevailing onshore flow in southeast China. The fall peak represents a return to the eastward transport from source regions that are less active than in spring. The model captures the observed seasonal cycle, although simulated values are low compared with the climatology, particularly in winter when snow suppresses dust mobilization in the model.

In the central Pacific, Midway and Oahu show a spring maximum, associated with Asian outflow, and a lull in summer. Simulated values fall generally within the observed range at Midway, and the model reproduces the springtime peak at midway in 2001, when concentrations exceed twice the climatological mean. The simulation is biased low at Oahu in January and February, similar to Cheju.

Export of African dust and transatlantic transport is illustrated using the remaining sites shown in Fig. 4. Sal Island and Izania (Tenerife) show monthly mean total dust values of between 10 and $60\,\mu g\,m^{-3}$ for most of the year. Sal Island shows a peak in February, whereas Izania shows higher values in summer, reflecting a seasonal northward shift of African dust outflow (Prospero et al., 2002). The model shows skill in representing these characteristics, although the model is biased high at Sal Island for most of the year. Barbados, Miami, and Bermuda see strongest African dust influence in summer. The simulation captures the seasonal cycle at Barbados, shows a summertime peak at Bermuda, but misses the observed summertime peak at Miami, for which 2001 data are shown. This is due to a known problem of excessive wet deposition associated convective in GEOS-3 meteorological fields off the Florida coast (Park et al., 2006).

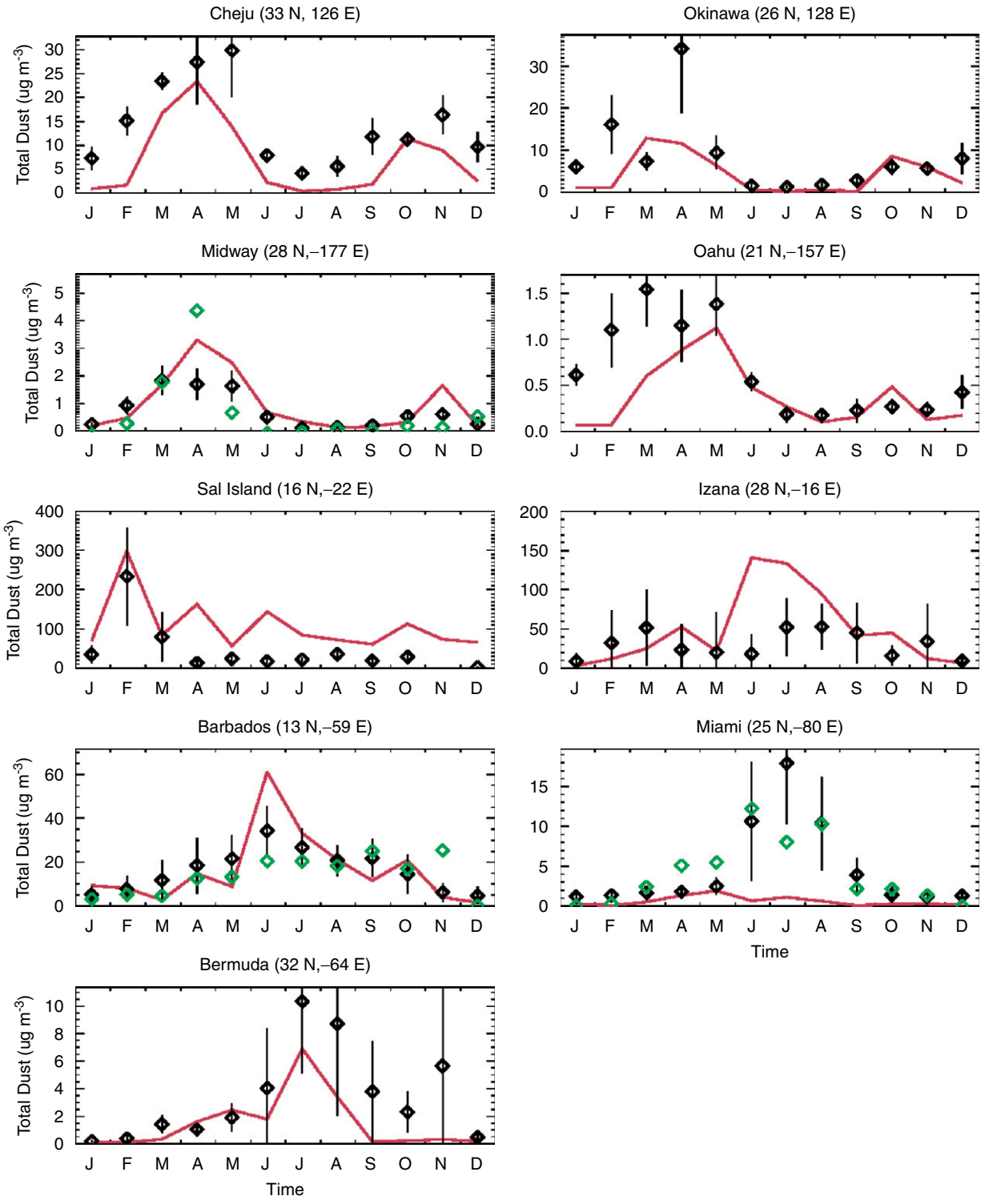

Fig. 3. Observed (black diamonds) monthly mean dust concentrations at selected N.H. sites from the U. Miami climatology ($\mu g\,m^{-3}$) with standard deviations (whiskers). Observations (green diamonds) and simulated values for 2001 (red lines) are also shown. Note differences in scales between panels.

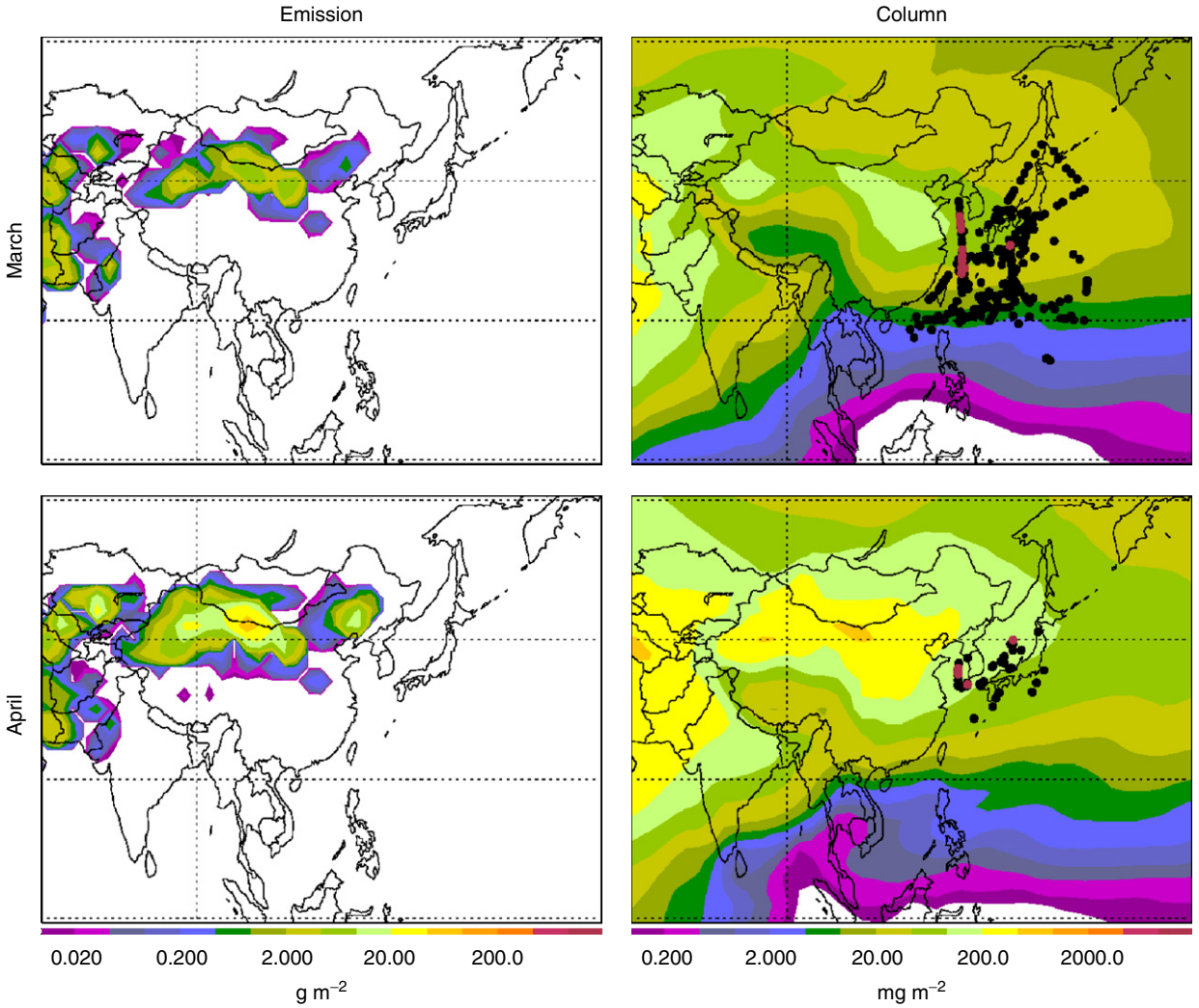

Fig. 4. Simulated monthly dust emission ($g\,m^{-2}month^{-1}$) and mean column mass ($mg\,m^{-2}$) for March (top) and April (bottom) 2001. Black symbols show the locations of dust measurements in TRACE-P (March) and ACE-Asia (April). Red symbols show observed occurrences of dust measurements above $100\,\mu g\,m^{-3}$.

4.2. *Aircraft observations of Asian outflow to the Pacific*

Aircraft measurements of Asian dust outflow to the Pacific were made in spring 2001 by the TRACE-P and ACE-Asia campaigns. For TRACE-P (Jacob et al., 2003), based in Hong Kong and Tokyo, we use bulk measurements of Ca^{2+} and Na^{+} from the DC8 aircraft (Dibb et al., 2003) to diagnose the mineral dust mass following Jordan et al. (2003). We restrict our comparison to data collected off the Asian eastern seaboard west of 150°E. For ACE-Asia campaign (Huebert et al., 2003), based in southern Japan, we use Ca^{2+} and Na^{+} data from the total aerosol sampler (TAS) aboard the C-130 aircraft (Kline et al., 2004; Huebert et al., 1998), and similarly convert to dust concentration following Jordan et al. (2003). Chin et al (2004) used TAS data to assess their simulation of this period. For both TRACE-P and ACE-Asia the model is sampled at the location and time of the aircraft observations.

Fig. 4 shows simulated dust emission and monthly mean column mass over East Asia and downwind for March and April 2001. Black symbols show the locations of the measurements. Red symbols indicate observed dust above $100\,\mu g\,m^{-3}$ at standard conditions ($T = 298\,K$,

$p = 1013$ hPa). March shows active source regions in the Gobi and Taklimakan deserts, and also in the Horqin region of northeast China (Gong et al., 2003). April shows marked intensification in these regions, reflecting in part a major dust storm on 6–8 April (Liu et al., 2003; Takemura et al., 2002; Jaffe et al., 2003; Szykman et al., 2003). April shows extensive outflow across Japan to the North Pacific, and the aircraft observations are well placed to sample the dust outflow.

Fig. 5 shows the altitude distribution of mineral dust from TRACE-P and ACE-Asia, together with model results sampled along the aircraft flight tracks. Corresponding scatter plots of the data are also shown. The model shows skill in simulating the vertical structure of the observed dust. While the model underestimates highest dust values in the boundary layer, it does better in the free troposphere (taken to be above 850 hPa), which drives transpacific transport. For TRACE-P the model was essentially unbiased in the free troposphere (mean bias of $-0.5\,\mu g\,m^{-3}$, -8%), with an rms difference of $16.1\,\mu g\,m^{-3}$. For ACE-Asia, mean dust observations were almost 10 times larger than in March, while simulated mean values were only four times bigger, leading to a mean bias above 850 hPa of $-36\,\mu g\,m^{-3}$ (-70%), and an rms difference of $91\,\mu g\,m^{-3}$. Nevertheless, the simulation of TRACE-P and ACE-Asia data offers us some confidence that the model represents the increasing Asian dust sources and transpacific transport in spring 2001.

5. Surface dust concentrations in North America

We now compare the model results with observations from the IMPROVE network. Fig. 6 shows simulated and observed seasonal mean concentrations of fine dust at IMPROVE stations for 2001. Overseas and domestic (North American) contributions are resolved using results from a simulation in

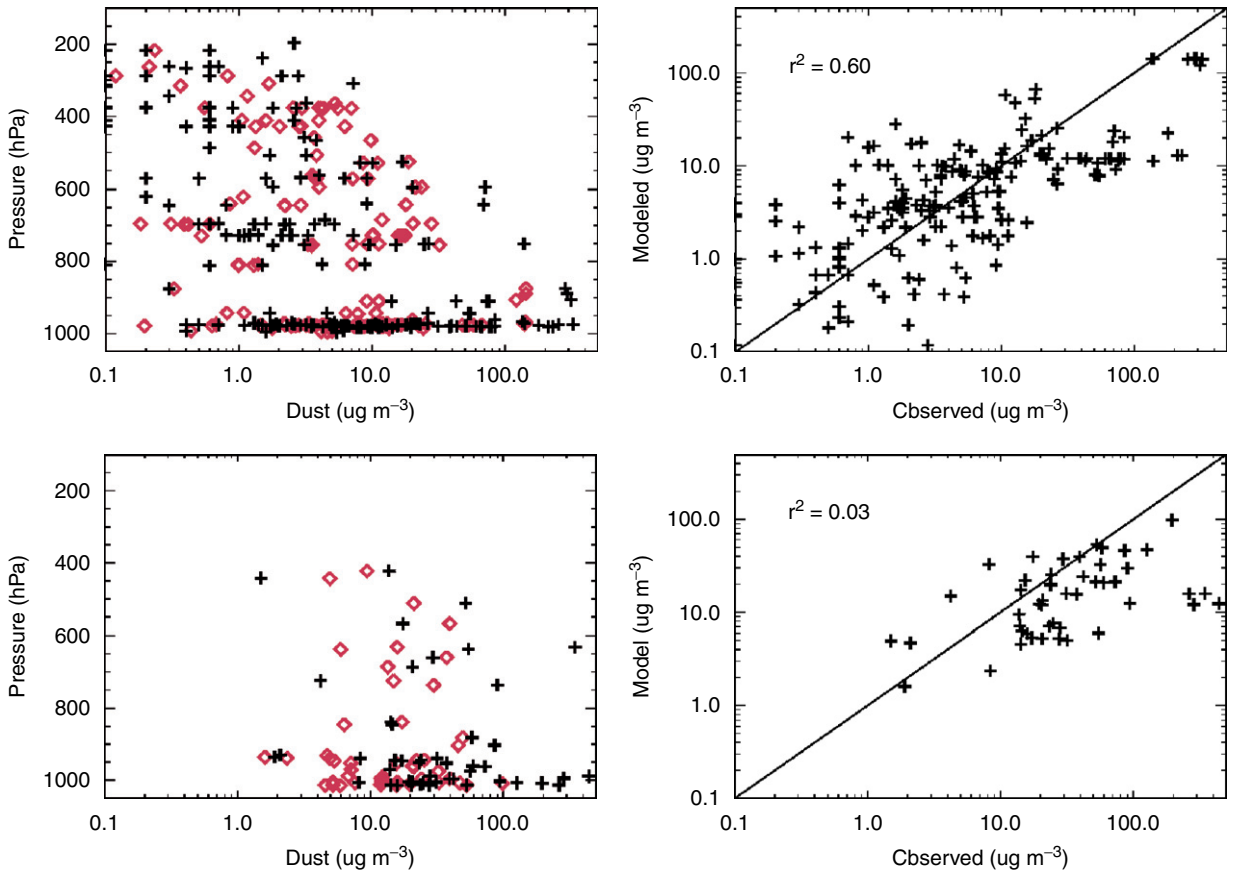

Fig. 5. Altitude distribution of mineral dust offshore from East Asia in spring 2001. Aircraft observations (black crosses) from TRACE-P (top) and ACE-Asia (bottom) are compared with model results (red diamonds) sampled along the flight tracks. Scatter plots are also shown.

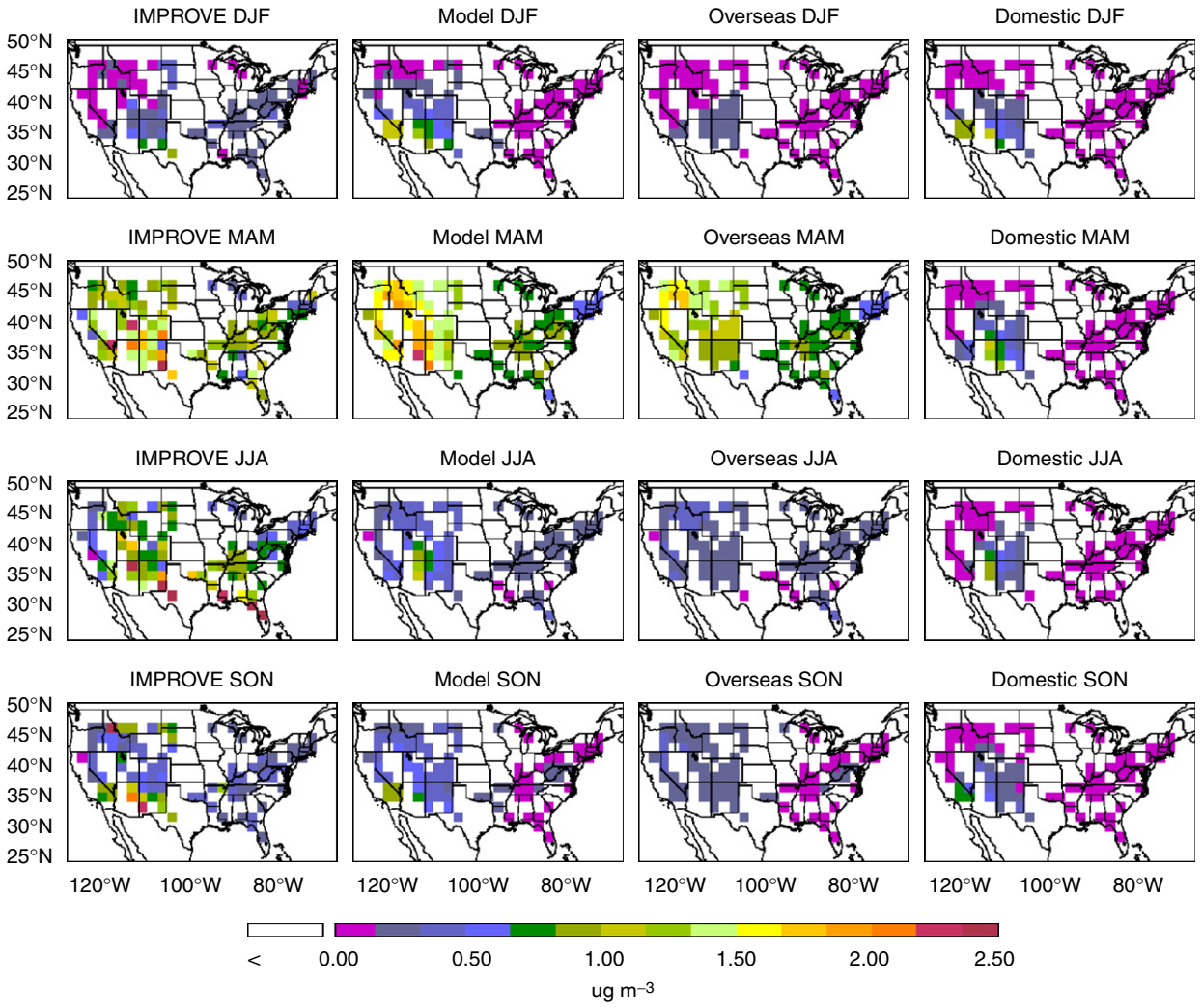

Fig. 6. Simulated and observed seasonal mean concentrations of fine dust (<2.5 μm) mass (μg m^{-3}) at IMPROVE stations for 2001. Rows 1–4 are for DJF, MAM, JJA, and SON respectively. Observations are spatially averaged over the 2° × 2.5° model grid. Simulated overseas and domestic (North American) contributions are shown in columns 3 and 4. Note: Color scale saturates at 2.5 μg m^{-3}; larger values appear red.

which North American emissions are excluded. IMPROVE observations are 24-h averages sampled every three days and we sample the model accordingly. Observed seasonal means are constructed by averaging the data for IMPROVE sites within each model grid box. Nevertheless, comparing localized observations with model results that are representative of a much larger area is inherently problematic. Fig. 7 shows individually observed and simulated time series at selected IMPROVE sites: Lava Beds is representative of high-altitude northwest sites; Great Smoky Mountains is an eastern Appalachian site; Guadalupe is a southwestern site close to regional dust sources.

Winter (DJF) is the seasonal minimum in fine dust at the IMPROVE sites (Van Curen and Cahill, 2002), with concentrations generally below 0.3 μg m^{-3}. Higher values in the southwest are due to domestic sources. The model is biased high in the southwest and low in the east, but values are small. Overseas influence in the model is below 0.15 μg m^{-3} at most locations.

Spring (MAM) is by contrast the seasonal maximum in dust across the continental United States. Largest values are found in the west, with seasonal means up to 3 μg m^{-3}, but dust is also elevated at eastern sites with 75% of sites showing seasonal means above 0.7 μg m^{-3}. This nationwide

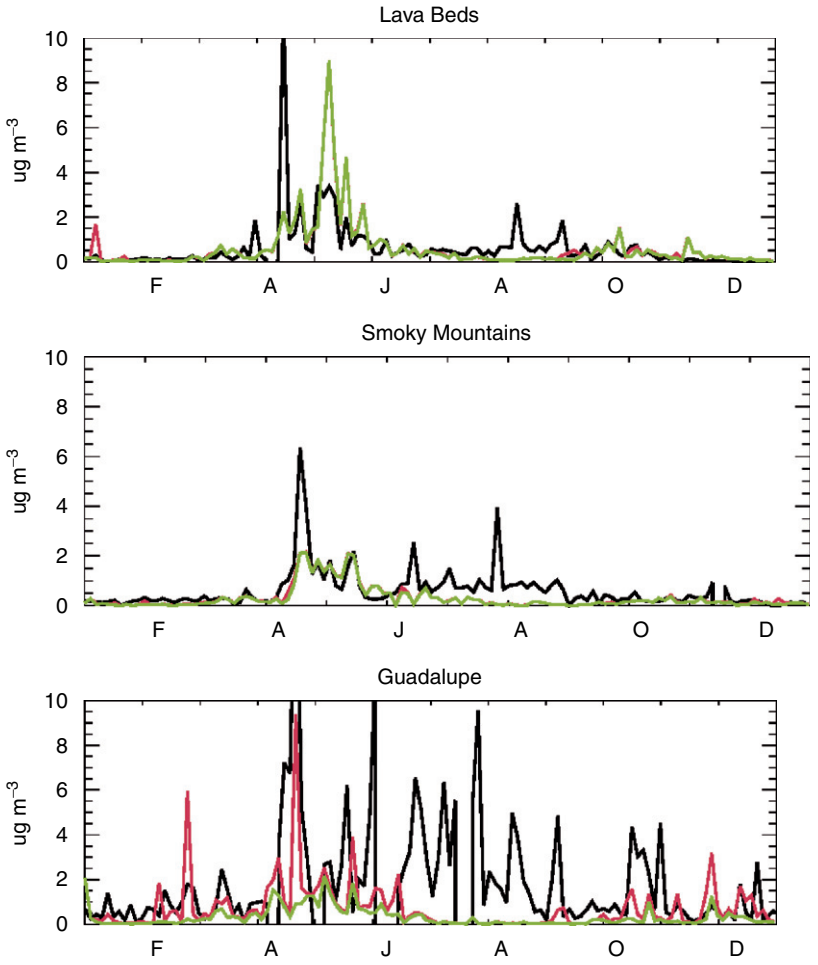

Fig. 7. Observed (black) and simulated (red) fine dust concentrations ($\mu g\,m^{-3}$) at Lava Beds, Great Smoky Mountains and Guadalupe IMPROVE sites for 2001. Simulated overseas contributions (green) are overlaid.

enhancement in spring is due principally to transpacific transport events in April and May (Jaffe et al., 2003; Szykman et al., 2003; Takemura et al., 2002; DeBell et al., 2004; Price et al., 2003), which appears as spikes of fine dust at IMPROVE sites (Fig. 7). Observed Al/Ca ratios of 1–2 (not shown) are consistent with an Asian origin for the dust (Van Curen and Cahill, 2002). The model captures the nationwide springtime enhancement, and attributes up to $2\,\mu g\,m^{-3}$ in the northwest to transpacific transport, although simulated values are high here because a simulated transpacific dust event in early May was twice as large as observed (see Lava Beds, Fig. 7). Domestic sources contribute 10–60% in southwestern locations, while in the east the model attributes 95% of fine dust to transpacific transport, with an overall 10% low bias. The model captures the timing of peaks of transpacific dust influence and indicates that the Asian dust presence persists in spring (Fig. 7). The model shows no impact from African dust over the continental US during spring, but attributes the observed seasonal mean of $1.7\,\mu g\,m^{-3}$ at Virgin Islands (not shown) to African dust.

North African dust peaks during the summer months (JJA) in Florida and along the Gulf Coast. Observed seasonal mean concentrations for JJA 2001 approach $2\,\mu g\,m^{-3}$ along the Gulf coast and are enhanced in the Appalachians and at east coast sites (75% of values exceed $0.5\,\mu g\,m^{-3}$). North African dust is evident at Great Smoky Mountains from June and July (Fig. 7), where Al/Ca ratios reach 3.8, characteristic of a Saharan origin (Perry et al, 1997). Domestic sources are active in the

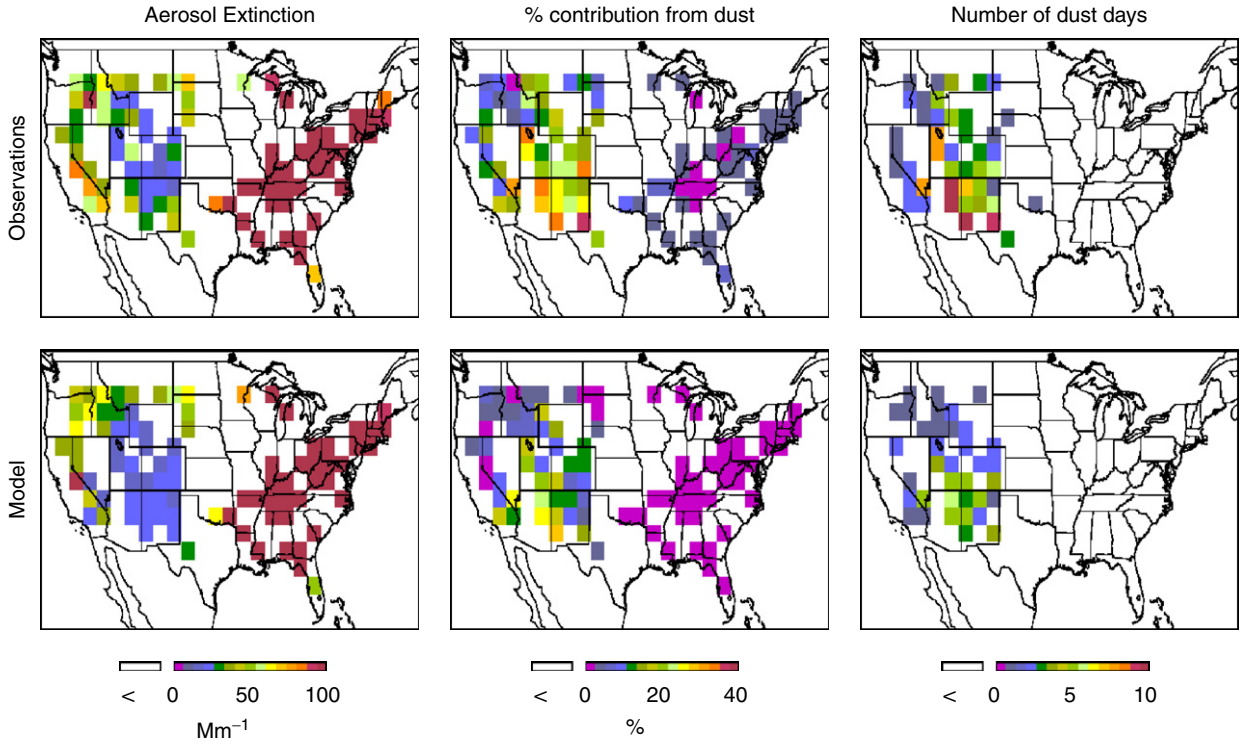

Fig. 8. Aerosol extinction statistics for the worst 20% visibility days at individual IMPROVE sites for 2001, averaged over the $2^\circ \times 2.5^\circ$ model grid, The top panels show mean aerosol extinction observations on those days, percentage contribution of dust to aerosol extinction, and the number of "worst dust days" (Kavouras et al., 2006), when dust contributes most of the aerosol extinction. The bottom panels show the corresponding results from the model.

southwest during the summer, e.g., at Guadalupe that is subject to regional dust sources in west Texas and northern Mexico, and shows peaks of fine dust approaching $10\,\mu g\,m^{-3}$ (Fig. 8) and seasonal means exceeding $3.0\,\mu g\,m^{-3}$. The model shows a small overseas influence in summer (JJA) over continental US transpacific influence peaks in the northwest with seasonal mean values of up to $0.4\,\mu g\,m^{-3}$. Van Curen and Cahill (2002) estimated an Asian influence of $0.5\,\mu g\,m^{-3}$ in summer at high-altitude western sites. The model is biased 50% low overall at western sites, but we attribute this to an underestimation of domestic emissions. The model fails to represent strong dust activity at Guadalupe in summer (Fig. 7), where only a small amount of overseas dust is evident. Simulated emissions are weak in the southwest in summer because the model resolved winds rarely reach the mobilization threshold. Much of the dust may be driven by dry convection or small-scale instabilities, e.g., dust devils (e.g., Gillette and Sinclair, 1990), that are not represented in the model. Cakmur et al. (2004) find that including a dust source from dry convection increases summertime emissions in the Northern Hemisphere and improves comparisons with satellite aerosol optical depths. Traffic on unpaved roads and agricultural activity may also contribute at western arid locations (Kavouras et al., 2006). The model fails to capture African influence at eastern sites because of excessive convective wet deposition off the east coast of Florida, as discussed previously.

In fall (SON) the African influence moves south and domestic sources in the west are more muted than in summer. The model shows a transpacific dust influence similar in fall as in summer with seasonal mean values approaching $0.4\,\mu g\,m^{-3}$ at western sites. The model is biased 25% low in the west and 50% in the east.

6. Implications for visibility impairment and the RHR

The US EPA (2003) RHR requires states to achieve a linear decrease in visibility impairment in their natural areas starting in 2004 and toward an endpoint of "natural visibility conditions" by 2064.

Visibility is measured as the logarithm of light extinction, and linear improvement is to be applied to the 20% worst visibility days. The EPA provides default estimates for natural concentrations of aerosol components to define the natural visibility endpoint. For fine dust ($<2.5\,\mu m$ diameter) and coarse mass ($>2.5\,\mu m$) these are 0.5 and $3.0\,\mu g\,m^{-3}$, respectively, nationwide. As seen in Fig. 6, however, there are large regional as well as seasonal differences.

Here, we consider the transpacific impact of mineral dust on visibility impairment at the IMPROVE sites during 2001. First, we identify the 20% worst visibility days for 2001 using IMPROVE data. We follow Kavouras et al. (2006) in defining "worst dust days" as the subset of the 20% worst visibility days for which dust (fine plus coarse mass) is the principal contributor to aerosol extinction. We then diagnose the 20% worst visibility days in the model and the corresponding worst dust days. To do this we have combined the results of our dust simulation with GEOS-Chem ($1^\circ \times 1^\circ$) model results for sulfate, nitrate, elemental carbon (EC), and organic carbon mass (OMC) aerosol at the IMPROVE sites for 2001 (Park et al., 2006). Park et al. showed that the model captures observed spatial distributions of the annual mean ($R^2 = 0.88$) and standard deviation ($R^2 = 0.66$) of daily visibility impairment at IMPROVE sites for 2001. Their simulation did not include dust. Here we add the dust component and distinguish the transpacific contribution on worst dust days.

We compute aerosol extinction, b_{ext}, at the IMPROVE sites using the formula recommended by the EPA (2003), which uses dry mass concentrations of individual aerosol components:

$$b_{ext} = 3f(RH)[(NH_4)_2SO_4 + NH_4NO_3] + 4[OMC] + 10[EC] + [soil] + 0.6[CM], \quad (6)$$

where f(RH) is a correction factor for hygroscopic growth as a function of relative humidity. For the model results, we take coarse mass (CM) = total−fine dust mass.

Fig. 8 shows observed mean aerosol extinction at the IMPROVE sites for the worst 20% visibility days in 2001, the contribution of dust (coarse + fine mass) to aerosol extinction on the worst visibility days, and the number of worst dust days at IMPROVE sites in 2001. Corresponding results from the model are also shown. Fig. 8 shows a large difference in aerosol extinction between the eastern and western US, reflecting large anthropogenic influences (mostly sulfate) in the east—see Park et al. (2006) for a detailed discussion of the model results. Dust contributes less than 10% to aerosol extinction in the east on the worst visibility days, but up to 43% in the west. The observation indicate 1–12 worst dust days at western sites, none in the east, for a total of 169 worst dust days at 44 locations. The model shows skill in reproducing the spatial pattern of aerosol extinction and the percent contribution of dust to aerosol extinction on the 20% worst visibility days. The model shows 89

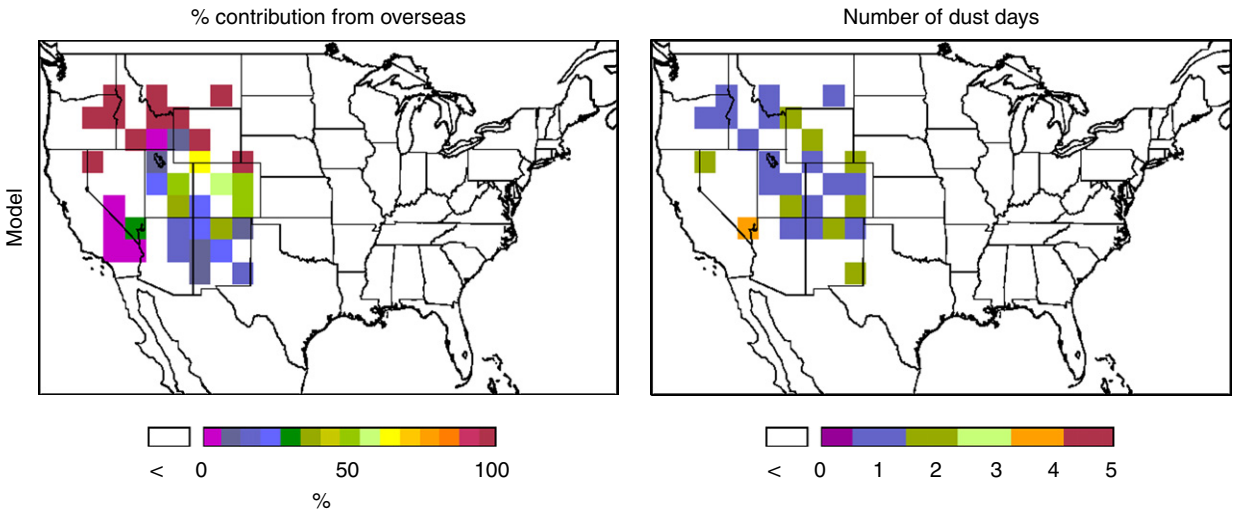

Fig. 9. Simulated overseas contribution to dust extinction for model worst dust days (%), and the number of model worst dust days attributed to transpacific transport.

worst dust days at 36 western locations, lower than observed, in large part because it underestimates coarse mass from summertime domestic sources. Coarse mass contributes between 50% and 80% to dust extinction at IMPROVE sites on observed worst dust days (not shown). As discussed above, parameterization of sub-grid-scale sources could reduce the underestimate of this coarse domestic component.

Fig. 9 shows the percentage of overseas contribution to dust extinction on the model worst dust days, and the number of model worst dust days attributed to overseas sources. Overseas sources contribute up to 100% to dust extinction on worst dust days in the northwest, and are responsible for typically 1–2 of the worst dust days at western sites. The model indicates that transpacific transport accounts for 41% (37 of 89) of worst dust days at western locations in 2001. This ratio is higher than that found by Kavouras et al. (2006), who attributed 63 of 203 (31%) worst dust days at western sites in 2001 to Asian sources.

7. Conclusions

We implemented a dust scheme in the GEOS-Chem global chemical transport model, and used it to assess the impact of transpacific dust influence on surface aerosol concentrations in the United States in 2001. We used two standard dust mobilization schemes—GOCART (G04) and DEAD (Z03)—but had issues with both for simulating US observations. GOCART yielded prolonged emissions, which we attribute to an insufficient wind threshold. DEAD generated excessive emissions over the northern plains in fall and early spring due to seasonally low LAI. We argue that LAI does not account for senescent or leafless ground cover, and land management practices aimed at soil erosion mitigation. We found that combining the entrainment scheme of DEAD with the topographic source from GOCART overcame some negative characteristics, which we encountered with each scheme individually.

Using the combined scheme the model captured much of the amplitude and seasonal cycle in dust climatologies at surface sites in the Northern Pacific. The model captured the springtime peak off the Asian coast and in the central Pacific. Simulated outflow of Asian dust in the free troposphere to the Northern Pacific is found to be unbiased in March compared to observations made from aircraft, although April values are underestimated.

We estimate the transpacific contribution of dust to aerosol concentrations over North America in 2001. The model captures the nationwide enhancement and spatial pattern of Asian dust over the United States in spring 2001. In addition, the model indicates that the transpacific contribution persists beyond springtime. We find that transpacific transport accounts for seasonal median fine dust ($<2.5\,\mu m$) concentrations of 0.12, 1.2, 0.25, and $0.25\,\mu g\,m^{-3}$ for DJF, MAM, JJA, and SON, respectively, in the western United States, with contributions 30–50% lower in the east.

We use the model to estimate the impact of transpacific transport of dust on visibility impairment in the US and implications for EPA RHR goals. We find that transpacific transport accounted for 41% of worst dust days (the subset of the 20% worst visibility days when dust was the dominant aerosol component) at western locations in 2001. Although meteorology controls the interannual variability in Asian dust emission and transport (Zhang et al., 2003), continued expansion of Asian dust source regions (Gong et al., 2004) could lead to future increased contributions from Asian dust over the United States.

Acknowledgments

We thank P. Ginoux and C. Zender for providing us with the dust mobilization codes, and for their advice in their implementation. We thank D. Savoie and J. Prospero for providing U. Miami data, B. Huebert, J. Dibb, and the ACE-Asia and TRACE-P science teams, Bret Schichtel and the IMPROVE team. Thanks to R. Miller for many helpful suggestions, and to M. Chin, P. Colarco, N. Mahowald, T. VanCuren, and I. Kavouras, for advice and discussions. The Electric Power Research Institute, the EPA STAR Program, and the NASA Langley Research Center Advanced Study Program supported this work.

References

Bey, I., et al., 2001. Global modeling of tropospheric chemistry with assimilated meteorology: model description and evaluation. Journal of Geophysical Research 106 (D19), 23073–23096.

Cakmur, R.V., Miller, R.L., Torres, O., 2004. Incorporating the effect of small-scale circulations upon dust emission in an

atmospheric general circulation model. Journal of Geophysical Research 109, D07201.

Cakmur, R.V., et al., 2006. Constraining the magnitude of the global dust cycle by minimizing the difference between a model and observations. Journal of Geophysical Research 111, D06207.

Carmichael, G.R., et al., 1996. variation of aerosol composition at Cheju Island, Korea. Atmospheric Environment 1352–2310 (95), 00230–002308.

Chin, M., et al., 2004. Aerosol distribution in the Northern Hemisphere during ACE-Asia: results from global model, satellite observations, and Sun photometer measurements. Journal of Geophysical Research 109, D23S90.

Clarke, A.D., et al., 2004. Size distributions and mixtures of black carbon and dust aerosol in Asian outflow: physio-chemistry, optical properties and implications for CCN. Journal of Geophysical Research 109, D15S09.

DeBell, L.J., et al., 2004. Asian dust storm events of spring 2001 and associated pollutants observed in New England by the Atmospheric Investigation, Regional Modeling, Analysis and Prediction (AIRMAP) monitoring network. Journal of Geophysical Research 109, D01304.

Dentener, et al., 1996. Role of mineral aerosol as reactive surface in the global troposphere. Journal of Geophysical Research 101 (D17), 22689–22889.

Dibb, J., et al., 2003. Aerosol chemical composition in Asian continental outflow during TRACE-P: comparison to PEM-West B. Journal of Geophysical Research 108 (D21), 8815.

Dockery, D.W., et al., 1993. An association between air pollution and mortality in six US cities. New England Journal of Medicine 329 (24), 1753–1759.

Fung, et al., 2000. Iron supply and demand in the upper ocean. Global Geochemistry Cycle 14 (1), 281–295.

Gillette, D.A., Passi, R., 1988. Modeling dust emission caused by wind erosion. Journal of Geophysical Research 93, 14,233–14,242.

Gillette, D.A., Sinclair, P.C., 1990. Estimation of suspension of alkaline material by dust devils in the United States. Atmospheric Environment 24A (5), 1135–1142.

Ginoux, P., et al., 2001. Sources and distributions of dust aerosols simulated with the GOCART model. Journal of Geophysical Research 106 (D17), 20255–20274.

Ginoux, P., et al., 2004. Long-term simulation of global dust distribution with the GOCART model: correlation with North Atlantic oscillation. Environmental Modeling and Software 19, 113–128.

Gong, S.L., et al., 2003. Characterization of soil dust aerosol in China and its transport and distribution during 2001 ACE-Asia: 2. Model simulation and validation. Journal of Geophysical Research 108 (D9), 4262.

Gong, S.L., et al., 2004. Sensitivity of Asian dust storm to natural and anthropogenic factors. Geophysical Research Letters 31, L07210.

Huebert, B.J., et al., 1998. Filter and impactor measurements of anions and cations during the first aerosol characterization experiment (ACE 1). Journal of Geophysical Research 103 (D13), 16493–16510.

Huebert, B.J., et al., 2003. An overview of ACE-Asia: strategies for quantifying the relationships between Asian aerosols and their climatic impacts. Journal of Geophysical Research 108 (D23), 8633.

Husar, R.B., et al., 2001. Asian dust events of April 1998. Journal of Geophysical Research 106 (D16), 18317–18330.

Iversen, J.D., et al., 1976. Saltation threshold on Mars: the effect of interparticle force, surface roughness, and low atmospheric density. Icarus 29, 381–393.

Jacob, D.J., 2000. Heterogeneous chemistry and tropospheric ozone. Atmospheric Environment 34, 2131–2159.

Jacob, D.J., et al., 2003. The transport and chemical evolution over the Pacific (TRACE-P) aircraft mission: design, execution, and first results. Journal of Geophysical Research. 108, 9000.

Jaffe, D., et al., 1999. Transport of Asian air pollution to North America. Geophysical Research Letters 26 (6), 711–714.

Jaffe, D., et al., 2003. The 2001 Asian dust events: transport and impact on surface aerosol concentrations in the United States. EOS Transactions 84 (46), 501–516.

Jordan, C.E., et al., 2003. Chemical and physical properties of bulk aerosols within four sectors observed during TRACE-P. Journal of Geophysical Research 108 (D21), 8813.

Kavouras, I.G., et al., 2006. Assessment of the principal causes of dust-resultant haze at IMPROVE sites in Western United States. Report to Western Regional Air Partnership (ttp://coha.dri.edu/dust).

Kline, J., et al., 2004. Aerosol composition and size versus altitude measured from the C-130 during ACE-Asia. Journal of Geophysical Research 109, D19S08.

Liao, H., Yung, Y.L., Seinfeld, J.H., 1999. Effect of aerosols on tropospheric photolysis rates in clear and cloudy atmospheres. Journal of Geophysical Research 104, 23697–23707.

Liu, H., Jacob, D.J., Bey, I., Yantosca, R.M., 2001. Constraints from 210Pb and 7Be on wet deposition and transport in a global three-dimensional chemical tracer model driven by assimilated meteorological fields. Journal of Geophysical Research 106, 12109–12128.

Liu, M., et al., 2003. A high-resolution numerical study of the Asian dust storms of April 2001. Journal of Geophysical Research 108 (D23), 8653.

Luo, C., Mahowald, N.M., del Corral, J., 2003. Sensitivity study of meteorological parameters on mineral aerosol mobilization, transport and distribution. Journal of Geophysical Research 108 (D15), 4447.

Mahowald, N.M., et al., 2002. Understanding the 30-year Barbados desert dust record. Journal of Geophysical Research 107 (D21), 4561.

Mahowald, N.M., Rivera, G.D.R., Luo, C., 2004. Comment on "Relative importance of climate and land use in determining present and future global soil dust emission" by I. Tegen et al. Geophysical Research Letters 31, L24105.

Malm, W.C., et al., 1994. Spatial and seasonal trends in particle concentration and optical extinction in the United States. Journal of Geophysical Research 99 (D1), 1347–1370.

Malm, W.C., et al., 2000. Spatial and seasonal patterns and temporal variability of haze and its constituents in the United States: Report III, Cooperative Institute for Research, Colorado State University, Fort Collins, CO.

Marticorena, B., Bergametti, G., 1995. Modeling the atmospheric dust cycle: 1. Design of a soil-derived dust emission scheme. Journal of Geophysical Research 100, 16415–16430.

Meskhidze, N., et al., 2005. Dust and pollution: a recipe for enhanced ocean fertilization. Journal of Geophysical Research 110, D03301.

Park, R.J., et al., 2004. Natural and transboundary pollution influences on sulfate–nitrate–ammonium aerosols in the United States: implications for policy. Journal of Geophysical Research 109, D15204.

Park, R.J., Jacob, D.J., Kumar, N., Yantosca, R.M., 2006. Regional visibility statistics in the United States: Natural and transboundary pollution influences, and implications for the Regional Haze Rule. Atmospheric Environment 40 (28), 5405–5423.

Penner, J., et al., 2001. Aerosols, their direct and indirect effects. In: Houghton, et al. (Eds.), Climate Change 2001: The Scientific Basis, Contribution of Working Group I to the Third Assessment Report of the IPCC. Cambridge University Press, Cambridge.

Perry, K.D., et al., 1997. Long-range transport of North African dust to the eastern United States. Journal of Geophysical Research 102 (D10), 11225–11238.

Price, H.U., et al., 2003. Vertical profiles of O_3, aerosols, CO and NMHCs in the northeast Pacific during the TRACE-P and ACE-ASIA experiments. Journal of Geophysical Research 108 (D20), 8799.

Prospero, J.M., 1996. Saharan dust transport over the North Atlantic ocean and Mediterranean: an overview. In: Guerzoni, S., Chester, R. (Eds.), The Impact of Desert Dust across the Mediterranean. Kluwer Academic Publishers, Boston, MA, pp. 131–151.

Prospero, J.M., 1999. Long-term measurements of the transport of African mineral dust to the southeastern United States: implications for regional air quality. Journal of Geophysical Research 104 (D13), 15917–15928.

Prospero, J.M., et al., 2002. Environmental characterization of global sources of atmospheric soil dust identified with the NIMBUS 7 total ozone mapping spectrometer (TOMS) absorbing aerosol product. Reviews of Geophysics 40 (1), 2.1–2.31.

Seinfeld, J.H., Pandis, S.N., 1998. Atmospheric Chemistry and Physics. Wiley, New York, p. 1326.

Shinn, E.A., et al., 2000. African dust and the demise of Caribbean coral reefs. Geophysial Research Letters 27 (19), 3029–3032.

Sisler, J.F., 1996. Spatial and seasonal patterns and long term variability of the composition of the haze in the United States: an analysis of data from the IMPROVE network, Cooperative Institute for Research, Colorado State University, Fort Collins, CO, ISSN 0737-5352-32.

Sokolik, I.N., et al., 2001. Introduction to special section: outstanding problems in quantifying the radiative impacts of mineral dust. Journal of Geophysical Research 106 (D16), 18015–18028.

Szykman, J., et al., 2003. Impact of 2001 Asia dust event on particulate matter concentrations in the United States, US EPA National air quality and emissions trends report, 2003, pp. S1–S12.

Takemura, T., et al., 2002. Modeling study of long-range transport of Asian dust and anthropogenic aerosols from East Asia. Geophysical Research Letters 29 (24), 2158.

Textor, C., et al., 2006. Analysis and quantification of the diversities of aerosol life cycles within AeroCom. Atmospheric Chemical Physics 6, 1777–1813.

Tegen, I., Werner, M., Harrison, S.P., Kohfeld, K.E., 2004. Relative importance of climate and land use in determining present and future global soil dust emission. Geophysical Research Letters 31, L05105.

US EPA, 2003. Guidance for estimating natural visibility conditions under the regional haze rule. US Environmental Protection Agency, Publication No. EPA 454-B-03-005.

Van Curen, R., Cahill, T., 2002. Asian aerosols in North America: frequency and concentration of fine dust. Journal of Geophysical Research 107 (D24), 4804.

White, B.R., 1979. Soil transport by winds on Mars. Journal of Geophysical Research 84, 4643–4651.

Zender, C.S., Bian, H., Newman, D., 2003a. The mineral dust entrainment and deposition (DEAD) model: description and 1990s dust climatology. Journal of Geophysical Research 108 (D14), 4416.

Zender, C.S., Newman, D., Torres, O., 2003b. Spatial heterogeneity in aeolian erodibility: uniform, topographic, geomorphic and hydrologic erodibility. Journal of Geophysical Research 108 (D17), 4543.

Zhang, L., Gong, S., Padro, J., Barrie, L., 2001. A size-segregated particle dry deposition scheme for an atmospheric aerosol module. Atmospheric Environment 35, 549–560.

Zhang, X.Y., et al., 2003. Sources of Asian dust and role of climate change versus desertification in Asian dust emission. Geophysical Research Letters 30 (24), 2272.